16th World Conference on Earthquake, 16WCEE 2017
Santiago Chile, January 9th to 13th 2017
Paper N° 4010
Registration Code: S-Y1450185613

DYNAMIC ANALYSIS MODEL OF VISCOELASTIC DAMPERS CONSIDERING TEMPERATURE-RISE AND HEAT CONVECTION UNDER LONG DURATION LOADING

K. Kasai[(1)], D. Sato[(2)], and D. Osabel[(3)]

[(1)] Professor, Tokyo Institute of Technology, Japan, kasai.k.ac@m.titech.ac.jp
[(2)] Assoc. Professor, Tokyo Institute of Technology, Japan, sato.d.aa@m.titech.ac.jp
[(3)] Graduate Student, Tokyo Institute of Technology, Japan, osabel.d.aa@m.titech.ac.jp

Abstract

Viscoelastic dampers dissipate energy through shear deformation of the viscoelastic materials; generating heat within the material causing it to soften. Therefore, under long duration excitation such as long period and duration earthquake, as well as wind loading, heat conduction and convection can occur and control the rise of temperature. The writers previously proposed two analytical methods simulating these effects and frequency sensitivities. First method combines three-dimensional heat transfer analysis and static analysis using common finite element model of the damper to estimate its dynamic properties referring to inclination and fatness of the hysteresis loop. The properties are estimated for every cycle considering transient state, or only a cycle which represents steady state cycle. The second method combines one-dimensional heat transfer analysis and viscoelastic constitutive rule using fractional time-derivatives of stress and strain, and it calculates step-by-step the force-deformation time histories of the damper. The present paper applies the above two methods to investigate the dampers of different proportions causing changes in heat generation, conduction, and convection. The paper also proposes a modified algorithm for calculating fractional time-derivatives of stress and strain, i.e., an approximate method using uniform shear strain distribution at every step. The analytically obtained deformed shape of the viscoelastic material is almost a straight-line, suggesting to idealize a uniform shear strain distribution. This modified algorithm is sufficiently accurate and hold advantage over the original algorithm in calculation time. The analysis models in this study accurately predict the real behavior of a viscoelastic damper when subjected to long duration loadings.

Keywords: viscoelastic damper; fractional derivative; long duration loading, temperature rise, heat transfer

1. Introduction

1.1 Viscoelastic Dampers

Among the widely-used devices to control structural vibration, viscoelastic (VE) dampers (e.g. Fig. 1a) are recognized to have significant advantage. They can be used not only for wind but also for earthquake excitations. These devices work by dissipating energy through shear deformation of the VE material. In the process of energy dissipation, heat is generated within the VE material; softening it and affecting its dynamic mechanical properties. For long duration excitations, significant heat conduction and convection can occur and control the temperature-rise.

1.2 Short Duration and Long Duration Models

Fig. 1a shows a VE damper subjected to dynamic loading, where $F_d(t)$ and $u_d(t)$ are time-varying damper force and deformation, respectively. Heat is generated within the VE material causing the damper dynamic properties such as storage stiffness K'_d and loss stiffness K''_d (Fig. 1b) to decrease. The proposed short duration model (Fig. 2) by Kasai et al [1, 2] showed the effect of temperature-rise due to the dissipated energy, and it considers uniform temperature θ and shear strain γ within the VE material. This has been found to be accurate for a short

duration excitation (typical earthquake) because heat conduction and convection insignificantly occur in short period of time.

However, for long duration loading such as wind force, heat conduction and convection play significantly. Kasai et al [3] showed that these greatly affect the distributions of temperature and strain within the VE material. For a long duration model (Fig. 3), therefore, the temperature θ and shear strain γ are expressed as functions of time t and thickness direction coordinate z [3].

1.3 Objectives and Scope

Presented herein are the previously proposed two analytical methods of Kasai et al [3] which accurately simulate the effects of temperature-rise, conduction and convection, and frequency sensitivities of VE dampers. The first is a three-dimensional (3D) static analysis with heat transfer using finite element model of a damper. The second combines one-dimensional (1D) heat transfer analysis and viscoelastic constitutive rule using fractional time derivatives of stress and strain.

A modified algorithm of the 1D model analysis is proposed in this paper. It approximates uniform shear strain distribution in the VE material at every step. Different damper configurations were analyzed using all three methods to determine the effects of damper shapes and proportions in heat generation, conduction and convection were investigated using all these methods.

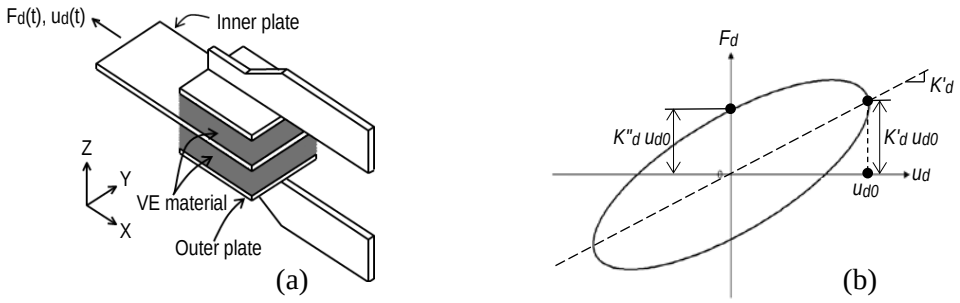

Fig. 1 – (a) Viscoelastic damper and its (b) hysteresis loop

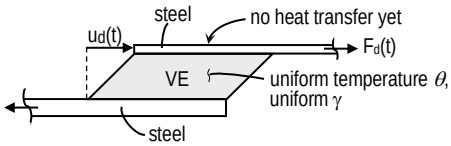

Fig. 2 – Short Duration Model

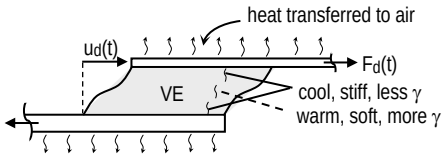

Fig. 3 – Long Duration Model

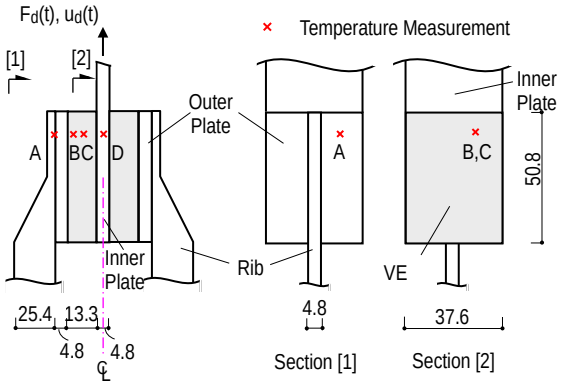

Fig. 4 – Test specimen & temperature measurement position. (unit: mm)

2. Long Duration Test

2.1 Test Specimen Description and Test Set-up

A long duration loading test of VE damper has been carried out to investigate its characteristics under long duration excitation and to validate the proposed analytical methods. Test specimen of a VE damper is shown in Fig. 4. Two VE material (3M-ISD110 type) laminations are bonded between the outer steel plates and inner steel

plate. Width of the VE laminations B = 37.6 mm, length L = 50.8 mm, and the thickness d_v = 13.3 mm. Total shear area A_v = 3,817 mm^2. Thickness of one steel plate d_s = 4.8 mm.

The test specimen was subjected to harmonic displacement of peak value $u_{d,max}$ = ±6.6 mm (±50% shear strain) at a frequency of 0.33 Hz. Loading duration was from t = 0 s to 3,000 seconds but temperature was continuously monitored up to 5,000 seconds. Ambient temperature was maintained at 24°C.

Temperature of VE damper was measured at four locations (Fig. 4). Measurement locations were: (A) at the surface of the outer plate; (B) and (C) at the 1/4 and 1/2 thickness points of the VE lamination, respectively, and; (D) at center of the inner plate.

2.2 Long Duration Loading Test Results

Fig. 5 shows the temperature time-history at each measurement locations indicated in Fig. 4. From initial temperature of 24°C, the damper temperature increases immediately upon loading and the change in temperature is different at each measurement location. Temperature-rise was sluggish until it was constant at each measurement point after t = 1,000 seconds. For cases of long duration loading such as in this study, temperature of VE damper attains steady-state at a certain time due to the effect of heat conduction and convection to-and-by the steel plates, and temperature no longer increases even if the VE damper is still subjected to loading. After 3,000 seconds when the loading has stopped, temperature at each measurement locations rapidly decreased to 24°C because the heat generation within the VE materials had stopped.

Fig. 6 shows the relationship of the damper force F_d and deformation u_d at the 1st, 100th and 1,000th cycles. Fig. 7 shows the change of damper storage stiffness K'_d and loss stiffness K''_d [2] which were obtained from damper hysteresis loop (Fig. 1b) and calculated every 20 cycles. As Fig. 7 indicates, K'_d and K''_d decreased immediately after loading. However, since the temperature became steady-state due to the effect of the heat conduction and convection as shown in Fig. 3, K'_d and K''_d became constant as well. Henceforth, this is an advantage of VE damper under long duration loading such as wind force.

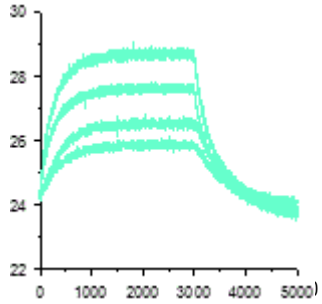

Fig. 5 – Temperature time-history

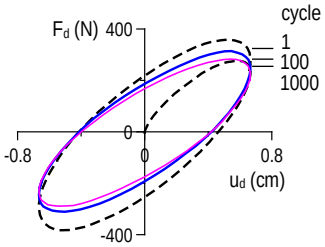

Fig. 6 – Force-deformation

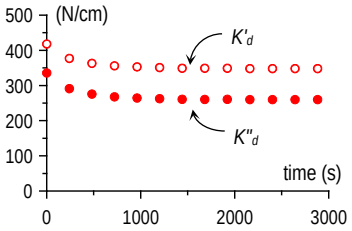

Fig. 7 – K'_d and K''_d

3. 3D-FEM Analysis

3.1 Static Analysis with Transient and Steady-State Heat Transfer Analyses

As stated above, it is essential to consider the heat conduction and convection to simulate the properties of VE damper under long duration loading. Hence, the variation of temperature and stiffness of VE damper having the temperature dependency is to be simulated.

G'_j and η_j, which are the storage shear modulus and the loss factor of the viscoelastic material at element j, are expressed in Eq. (1) [1, 2].

$$G'_j = G\frac{1+a_jb_j\omega^{2\alpha}+(a_j+b_j)\omega^{\alpha}\cos(\alpha\pi/2)}{1+a_j^2\omega^{2\alpha}+2a_j\omega^{\alpha}\cos(\alpha\pi/2)} \quad , \qquad \eta_j = \frac{(-a_j+b_j)\omega^{\alpha}\sin(\alpha\pi/2)}{1+a_jb_j\omega^{2\alpha}+(a_j+b_j)\omega^{\alpha}\cos(\alpha\pi/2)} \qquad (1a, b)$$

where, α = fractional derivative order; a_j, b_j and G = parameter of the fractional derivative. a_j and b_j are dependent on temperature θ_j, and these are expressed as follows:

$$a_j = a_{ref}\lambda_j^{\alpha}, \quad b_j = b_{ref}\lambda_j^{\alpha}, \quad \lambda_j = \exp\left[-p_1\left(\theta_j - \theta_{ref}\right)/\left(p_2 + \theta_j - \theta_{ref}\right)\right] \tag{2a-c}$$

Here, λ_j is called "shift factor"; a_{ref} and b_{ref} are values of a and b at reference temperature θ_{ref}, respectively. The parameters of the fractional derivative for ISD110 are: G = 6.516 N/cm^2; α = 0.609; a_{ref} = 0.0115 and b_{ref} = 21.157; θ_{ref} = 0.2°C, and; p_1 and p_2 are 19.5 and 80.2, respectively. The storage modulus for axial direction E'_j is expressed in Eq. (3) using the Poisson's ratio ν.

$$E'_j = 2G'_j(1+\nu) \tag{3}$$

The algorithm of the 3D-FEM analysis is shown as follows: The frequency ω, maximum damper deformation (amplitude) $u_{d,max}$, and initial temperature θ_j at element j are first set. Then G'_j, E'_j and η_j are calculated using Eq. (1) to (3).

Static analysis when the damper deformation is $u_{d,max}$ is carried out. The reaction force of the damper F'_d is then obtained. By multiplying the strain energy of the element j from the static analysis results by $2\pi\eta_j$, the energy dissipated per cycle $W_{d,j}$ is determined (Eq. (4)).

$$W_{d,j} = \pi\eta_j V_j\left\{\sum_{k=1}^{3} E'_j\,\varepsilon_{kk,j}^2 + G'_j\left(\gamma_{12,j}^2 + \gamma_{23,j}^2 + \gamma_{31,j}^2\right)\right\} \tag{4}$$

where V_j = volume of element j, $\varepsilon_{mn,j}$ and $\gamma_{mn,j}$ = strain at the center of the element. Then the damper storage stiffness K'_d and loss stiffness K''_d are calculated using Eq. (5). The heat generated per unit volume and unit time $\dot{Q}_j$ is expressed by Eq. (6), where T = period of 1 cycle.

$$K'_d = F'_d / u_{d,\max}, \quad K''_d = \left(\sum_j W_{d,j}\right) / \left(\pi u_{d,\max}^2\right) \tag{5a, b}$$

$$\dot{Q}_j = W_{d,j} / (V_j T) \tag{6}$$

After the damper displacement returned to zero, the amount of heat generated being calculated from Eq (6) is used for transient-state analysis which corresponds to one cycle of T seconds. Using the temperature result of the VE material, G'_j, η_j and E'_j in Eqs. (1) and (3) are recalculated for each element. For the next cycle, perform the static analysis for damper deformation of $u_{d,max}$. This will be repeated for the required number of cycles.

3.2 3D-FEM Model

The 3D-FEM model is shown in Fig. 8. As the model is symmetric with respect to the center of the inner plate, 3D-FEM is carried out by using half of this model. 3D coupled temperature-displacement solid elements (ABAQUS Ver. 6.4) are utilized in this model. The width of the VE lamination B is divided into 18 elements, the length L is divided into 18 elements, the thickness d_v is divided into 12 elements, and 8,260 elements are used for this damper model.

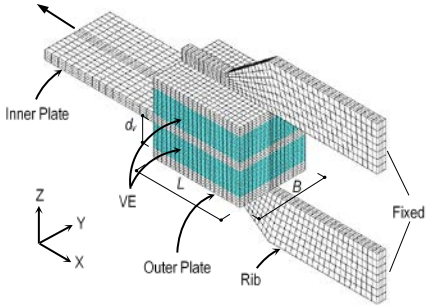

Fig. 8 – 3D-FEM Model

The inner plate is given the controlled displacement $u_{d,max}$ along X-direction. The end of the rib is fixed and the reaction force of VE damper F'_d can be obtained. The inner plate cannot move in Y- and Z-directions. The symmetric surface, the center of the inner plate, is set as insulation boundary condition. The ambient temperature θ_c = 24°C, same as the test condition.

The parameters used for the 3D-FEM model were: $(s\rho)_{steel}$ = 363.71 N/cm^2/°C, $(s\rho)_{VE}$ = 194.00 N/cm^2/°C, κ_{steel}= 43.128 N/s/°C, and κ_{VE}= 0.188 N/s/°C where κ = thermal conductivity, s = specific heat capacity, ρ = density. Heat transfer coefficients α_c were obtained by using a trial-and-error method, referring to Reference [4], and decided to use α_c = 0.25 N/s/cm/°C (1 N/s/cm/°C = 100 W/m^2/°C) for this study. This value describes the situation is between "free convection" and "forced convection" [3]. The Poisson's ratio for the VE material is 0.47, steel is 0.30, and Young's modulus of the steel is 2.05 x 10^7 N/cm^2.

3.3 Experimental Verification

Fig. 9 shows the result of the temperature and Fig. 10 are the K'_d and K''_d of the test and 3D-FEM analysis (transient and steady states) as mentioned above. Analytical results are in good agreement with the test results.

Temperature distribution calculated using 3D-FEM analysis is shown in Fig. 11. The VE material reached a maximum temperature of 29.1°C after 3,000 s. Temperature distribution in the Z-direction are different at each point whereas the temperature in the X-Y section is uniform except at the extreme portion of the surface.

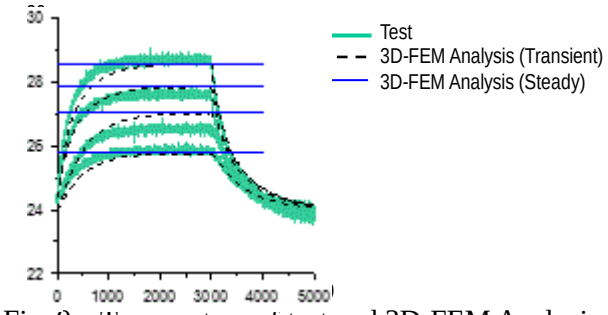

Fig. 9 – Temperature of test and 3D-FEM Analysis

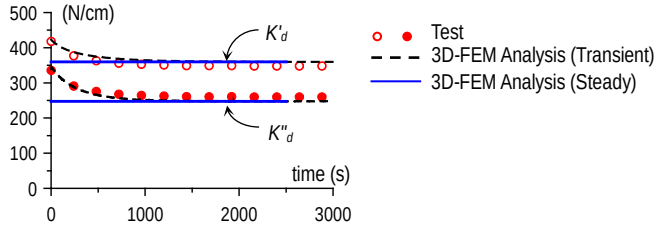

Fig. 10 – K'_d and K''_d of test and 3D-FEM Analysis

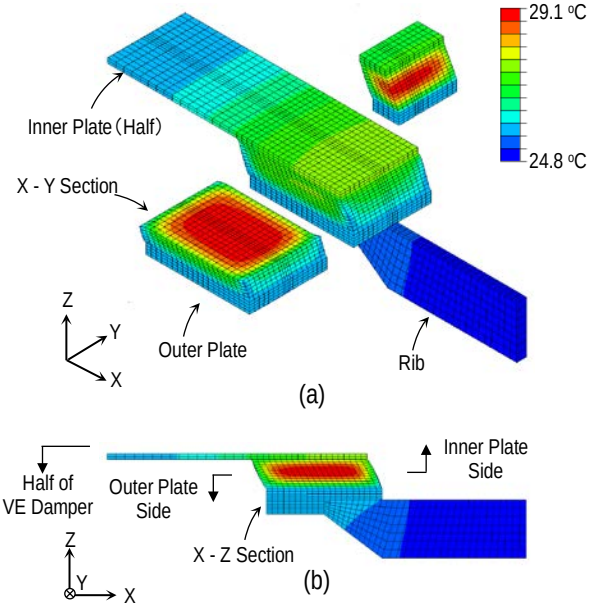

Fig. 11 – Temperature distribution at 3,000 sec

3.4 Effects of Damper Shapes and Proportions

As verified by the test results, the proposed 3D-FEM analysis method is accurate in predicting the properties of a VE damper under long duration loadings (Figs. 9 and 10). Using the same technique, different damper configurations (Figs. 12 and 13) were analyzed in order to determine the effects of damper shapes and proportions. The original damper (Fig. 8) is referred as "Damper 1" from this section onwards. Note that maximum shear strain of each damper is ±50%, thus, the $u_{d,max}$ for Damper 2 is ±6.6 mm while for Damper 3 is ±3.3 mm.

Temperature distribution of Dampers 2 and 3 using 3D-FEM analysis method are shown in Figs. 12 and 13. With similar VE material thickness, amount of heat generated for Dampers 1 and 2 are similar. However, with more surface area for heat dispersion to the air (See Table 1), accumulation of heat in the VE material in Damper 2 (Fig. 12) is lesser compared to Damper 1 resulting to slightly lower value of maximum temperature.

Moreover, the maximum temperature of Damper 3 is only 26.4°C (Fig. 13) which is significantly lower compared to Damper 1. This is due to lesser amount of heat generated from a thinner VE material.

Despite the difference in temperature, the distribution patterns for all the dampers are similar, i.e. uniform distribution in the X-Y section, and varying at each point in the Z-direction. This suggests that VE dampers can be treated as a one-dimensional (1D) heat transfer problem in the thickness direction (discussed in Section 4).

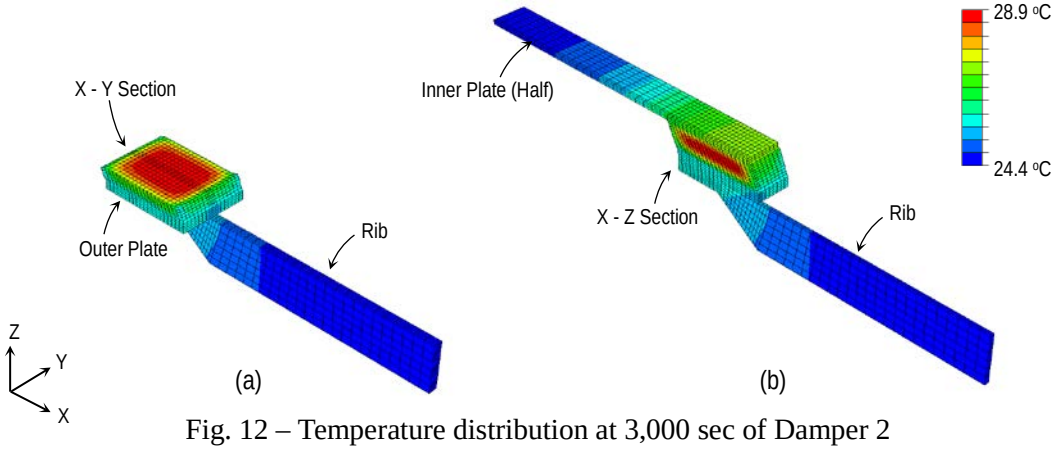

Fig. 12 – Temperature distribution at 3,000 sec of Damper 2
(Inner plate and rib are twice longer than Damper 1)

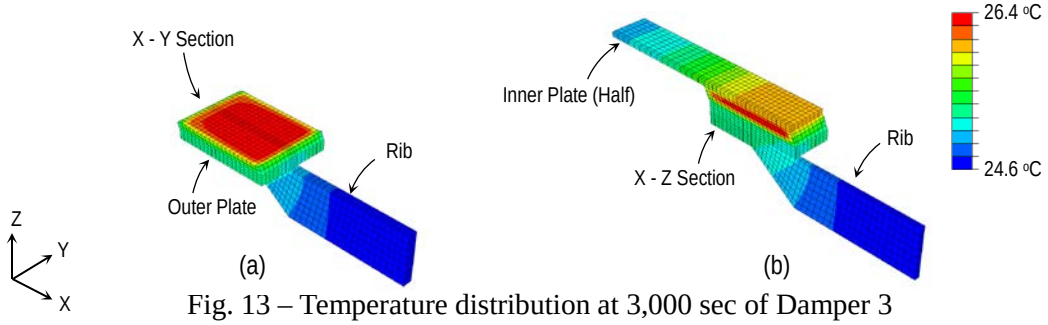

Fig. 13 – Temperature distribution at 3,000 sec of Damper 3
(VE material thickness is half of Damper 1)

Table 1 – Comparison of heat flow rates of different damper configurations

Damper	Comparison	Inner Plate	VE Side	Outer Plate	Rib	Total
1	Surface Area cm^2	41.84 (29.0%)	23.47 (16.3%)	25.07 (17.4%)	53.83 (37.3%)	144.21 (100.0%)
	Heat Flow N·cm/s	22.05 (35.4%)	14.43 (23.2%)	10.34 (16.6%)	15.46 (24.8%)	62.29 (100.0%)
2	Surface Area cm^2	79.47 (36.1%)	23.47 (10.7%)	25.07 (11.4%)	92.32 (41.9%)	220.33 (100.0%)
	Heat Flow N·cm/s	22.83 (34.1%)	14.99 (22.4%)	10.65 (15.9%)	18.50 (27.6%)	66.97 (100.0%)
3	Surface Area	41.84	11.47	25.07	53.83	133.54

	cm^2	(31.3%)	(8.8%)	(18.8%)	(40.3%)	(100.0%)
	Heat Flow N·cm/s	13.34 (35.3%)	4.97 (13.2%)	8.40 (22.2%)	11.09 (29.3%)	37.80 (100.0%)

4. 1D-Time History Analysis including Transient-State Heat Transfer

The non-linear model of a VE damper earlier proposed by Kasai et al [1, 2] considers heat generation only and reasonably accurate to simulate VE dampers under short duration loadings like an earthquake as heat conduction and convection effects are negligible. Thus, it will be called a "Short Duration Model' in this study.

Results of 3D-FEM analysis in Figs. 11 – 13 suggest that the temperature distribution inside the VE damper can be expressed by using one-dimensional (1D) heat transfer problem in the thickness direction. This chapter proposes a "Long Duration Model" which is a time-history analysis method combining one-dimensional heat transfer analysis and the viscoelastic constitutive rule using fractional time-derivatives of stress and strain. It will calculate step-by-step the force-deformation time-histories of a VE damper.

4.1 Formulation

Consider a VE damper (Fig. 14a) subjected to dynamic loading, where $F_d^{(n)}$ and $u_d^{(n)}$ are damper force and deformation at time step n, respectively. Fig. 14b is an example of discretizing the damper into elements for 1D-heat transfer analysis. Here, m is the total number of elements; j is node number with j_1 and j_2 being the end nodes of the VE material, and; d_j is the length of element j.

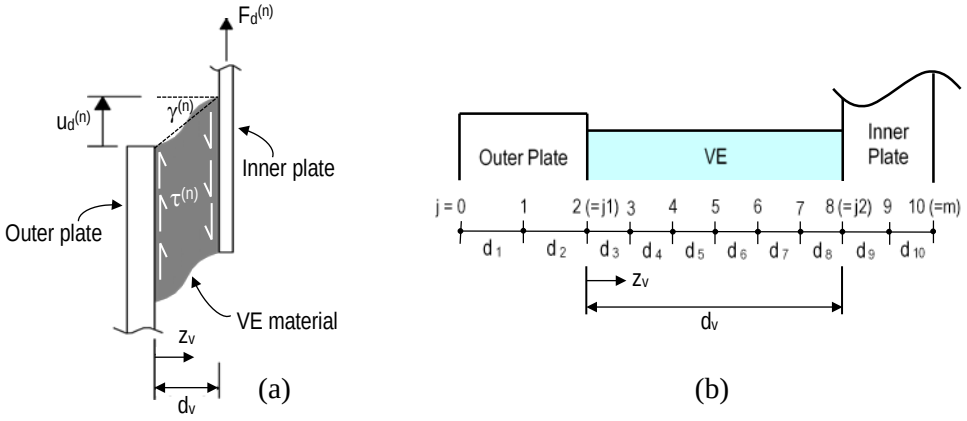

Fig. 14 – Damper model for 1D-heat transfer analysis with constitutive rule

When the n^{th} step damper deformation $u_d^{(n)}$ is known, the compatibility equation between the damper deformation $u_d^{(n)}$ and shear strain $\gamma_j^{(n)}$ can be expressed as Eq. (7). Here, $\zeta_{j_1} = d_{j_1+1}$, $\zeta_{j_2} = d_{j_2}$ and $\zeta_j = d_j + d_{j_1+1}$ when $j_1 < j < j_2$.

$$u_d^{(n)} = \frac{1}{2}\sum_{j=j_1}^{j_2} \zeta_j \gamma_j^{(n)} \tag{7}$$

Shear stress $\tau^{(n)}$ is uniform along the thickness direction by equilibrium rule. Since strain and temperature distribution are not uniform throughout the thickness of the VE material, the fractional derivative is written as:

$$\tau^{(n)} + a_j^{(n)} D^\alpha \tau^{(n)} = G\left[\gamma_j^{(n)} + b_j^{(n)} D^\alpha \gamma_j^{(n)}\right] \tag{8}$$

where $D^\alpha (=d^\alpha/dt^\alpha)$ is the fractional derivative operator of order α. All were described in Section 3.1, however, temperature-dependent constants a_j and b_j are calculated at every time step.

$$a_j^{(n)} = a_{ref}(\lambda_j^{(n)})^\alpha, \qquad b_j^{(n)} = b_{ref}(\lambda_j^{(n)})^\alpha, \qquad \lambda_j^{(n)} = \exp\left[-p_1\left(\theta_j^{(n)} - \theta_{ref}\right)/\left(p_2 + \theta_j^{(n)} - \theta_{ref}\right)\right] \tag{9a-c}$$

Considering step-by-step integration scheme, Eq. (8) is expressed as

$$\tau^{(n)} + a_j^{(n)} \sum_{i=0}^{N} w^{(i)} \tau^{(n-i)} = G\left[\gamma_j^{(n)} + b_j^{(n)} \sum_{i=0}^{N} w^{(i)} \gamma_j^{(n-i)} \right] \tag{10}$$

where Δt = time step size; N = number of integration step which, as suggested by Kasai et al [2], is 1.5T to consider until the 3rd frequency of building. Weight functions $w^{(i)}$ are given in Eq. (11) where Γ refers to gamma function.

$$\begin{aligned} &w^{(0)} = 1/\Gamma(2-\alpha)/(\Delta t)^{\alpha}, \qquad w^{(i)} = w^{(0)} \left\{ (i-1)^{1-\alpha} - 2i^{1-\alpha} + (i+1)^{1-\alpha} \right\}, \\ &w^{(N)} = w^{(0)} \left\{ (N-1)^{1-\alpha} - N^{1-\alpha} + (1-\alpha) N^{-\alpha} \right\} \end{aligned} \tag{11a-c}$$

Finally, time-step shear stress $\tau^{(n)}$ can be determined by combining Eqs. (7), (10) and (11).

$$\tau^{(n)} = \left\{ 2Gu_d^{(n)} - \sum_{j=j_1}^{j_2} \frac{\zeta_j \left(\tilde{A}_j^{(n)} - \tilde{B}_j^{(n)} \right)}{1 + b_j^{(n)} w^{(0)}} \right\} \Bigg/ \sum_{j=j_1}^{j_2} \frac{\zeta_j \left(1 + a_j^{(n)} w^{(0)} \right)}{1 + b_j^{(n)} w^{(0)}} \tag{12}$$

where

$$\tilde{A}_j^{(n)} = a_j^{(n)} \sum_{i=1}^{N} w^{(i)} \tau^{(n-i)}, \qquad \tilde{B}_j^{(n)} = G b_j^{(n)} \sum_{i=1}^{N} w^{(i)} \gamma_j^{(n-i)} \tag{13a, b}$$

Multiplying the shear stress $\tau^{(n)}$ by the shear area A_v gives us the damper force $F_d{}^{(n)}$ (Eq. (14)).

$$F_d{}^{(n)} = \tau^{(n)} A_v \tag{14}$$

The temperature-rise $\Delta\theta_j^{(n)}$ due to the energy dissipated $\Delta E_j^{(n)}$ for Δt at node j is expressed as:

$$\Delta\theta_j^{(n)} = \frac{1}{2} \left(\frac{\Delta E_j^{(n)}}{s_j \rho_j} + \frac{\Delta E_{j+1}^{(n)}}{s_{j+1} \rho_{j+1}} \right), \qquad \Delta E_j^{(n)} = \left(\tau^{(n)} + \tau^{(n-1)} \right) \left(\gamma_{j-1}^{(n)} - \gamma_{j-1}^{(n-1)} + \gamma_j^{(n)} - \gamma_j^{(n-1)} \right) / 4 \tag{15a, b}$$

where $\Delta E_{j_1}^{(n)} = \Delta E_{j_2+1}^{(n)} = 0$ because these are steel plate parts.

The temperature distribution of the VE damper $\theta_j^{(n+1)}$at (n+1) step is the sum of the temperature-rise due to the dissipated energy $\Delta E_j^{(n)}$ and the temperature rise and/or fall due to heat transfer $\hat{\theta}_j{}^{(n)}$ (Eq. (16)).

$$\theta_j{}^{(n+1)} = \Delta\theta_j{}^{(n)} + \hat{\theta}_j{}^{(n)}, \qquad \hat{\theta}_j{}^{(n)} = \sum_{k=0}^{m} x_{jk} \ \theta_k{}^{(n)} + y_j \tag{16a, b}$$

where Eq. (16b) expresses the simplified 1D-heat transfer equation solution [3].

4.2 Determination of Heat Transfer Coefficient

The heat transfer coefficients used in the 1D-long duration model are decided in order that the rates heat flow are the same as the 3D-FEM analysis results in Section 3. Therefore, the heat transfer coefficients $\alpha_{c,out}$ and $\alpha_{c,in}$ for the outer plate and inner plate sides, respectively, are expressed as follows:

$$\alpha_{c,out} = Q_{out} / \{ A_d (\theta_{out} - \theta_c) \}, \qquad \alpha_{c,in} = Q_{in} / \{ A_d (\theta_{in} - \theta_c) \} \tag{17}$$

where θ_c is the ambient temperature; A_d is the cross-sectional area (X-Y section) of the VE material; Q_{out} and Q_{in} are the heat flow rates at the outer plate and inner plate sides from the 3D-FEM analysis results (Table 1), respectively; θ_{out} and θ_{in} are the average surface temperature at the outer plate and inner plate sides obtained from the 3D-FEM analysis result, respectively. Then for Damper 1, $\alpha_{c,out}$ = 0.956 N/s/cm/°C and $\alpha_{c,in}$ = 0.524 N/s/cm/°C.

4.3 Experimental Verification

The proposed 1D-long duration model is verified using the experimental results of Damper 1 (Section 2). It is also compared with the result from the Short Duration Model [1, 2]. Fig. 15 shows the comparison of temperature and it can be seen that the long duration model agrees well with the test results, however, the short duration model results fail prematurely because it did not consider heat conduction and convection.

It is worth noting that the temperatures from the 1D-long duration model have better match with the test results (Fig. 15) as compared to analytical results of 3D-FEM model (Fig. 9). Such observation can be significantly seen at point D. However, this does not hold huge advantage with respect to dynamic properties of the VE damper because the temperature in the VE material (points B and C) for both models are similar to the test.

Comparisons of storage stiffness K'_d and loss stiffness K''_d between the test, long duration model and short duration model are shown in Fig. 16. Those calculated by the long duration model are in good agreement with the test results. On the other hand, results from short duration model show significant softening of the VE material because of overestimated temperature (Fig. 15).

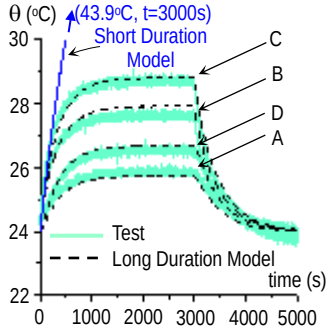

Fig. 15 – Comparison of temperature of Damper 1

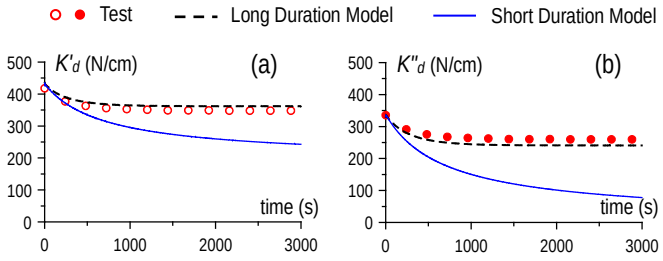

Fig. 16 – Comparison of K'_d and K''_d of Damper 1

4.4 Effects of Damper Shapes and Proportions

Table 2 indicates the heat transfer coefficients for the different damper configurations (Section 3.4) being calculated using Eq. (17). Damper 2 having the lengths of rib and inner plate being twice that of Damper 1, the heat transfer coefficients have increased. On the other hand, Damper 3 with VE material being half that of Damper 1, the coefficients of heat transfer have decreased. However, the ratios between $\alpha_{c,out}$ and $\alpha_{c,in}$ for the three damper configurations are close to each other.

Table 2 – Heat transfer coefficients

Damper	$\alpha_{c,out}$ (N/s/cm/°C)	$\alpha_{c,in}$ (N/s/cm/°C)	$\alpha_{c,out}/\alpha_{c,in}$
1	0.956	0.524	1.824
2	1.104	0.589	1.874
3	0.885	0.446	1.984

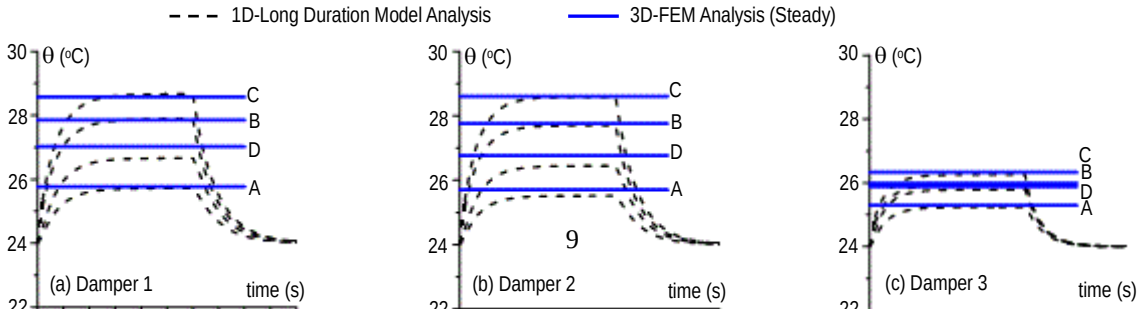

Fig. 17 shows the comparisons of temperature from the 1D-long duration model and those from 3D-FEM steady-state analysis (Section 3.4). As seen, the temperature in the VE materials portions (points B and C) for both models are in good agreement. As cited in Section 3.3, there is an observable difference in predicted temperature at point D from the models but this is not affecting the dynamic properties of the VE damper.

The force-deformation relations from the 1D-long duration model analysis were determined (Fig. 18). To accommodate the variations of damper deformations (Section 3.3), the horizontal axis for Fig. 18c (Damper 3) is scaled up by a factor of 2. Noticeably, Dampers 1 and 2 have significantly softened immediately after few cycles (50 cycles) as compared to Damper 3. After 1,000 cycles, the stiffness of Damper 3 has lowered insignificantly while Dampers 1 and 2 have drastically decreased. This is due to the varying amount of temperature increase for different damper configurations indicated in Fig. 17.

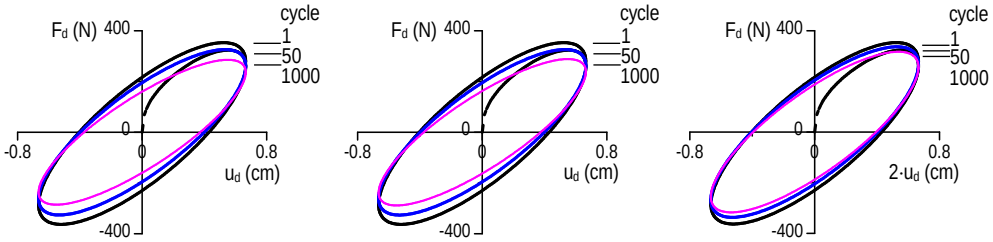

(a) Damper 1 (b) Damper 2 (c) Damper 3

Fig. 18 – Force-deformation relations from 1D-long duration model

5. Approximate Method Assuming Uniform Strain Distribution

5.1 Formulation

The 1D-detailed long duration (DLD) model accurately predicts lower temperature and less shear strain near the steel plate interface, and higher temperature and more shear strain at the inner locations (Fig. 19b). However, as Fig. 19c shows, analytically obtained deformed shape of the VE material of Damper 1 is almost straight, suggesting approximately uniform strain distribution.

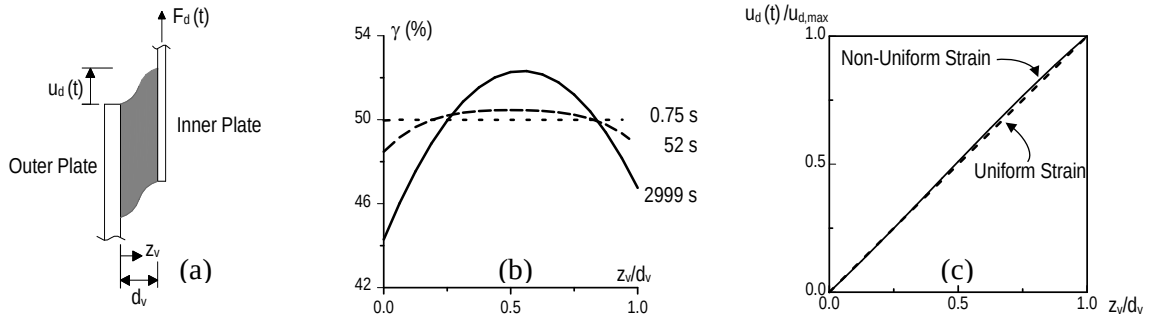

Fig. 19 – (a) VE damper as modeled for DLD model ; (b) Strain distribution of Damper 1, and; (c) Analytically obtained deformed shape of Damper 1 at t = 2999s

Therefore, a simplified long duration (SLD) model is proposed in this section idealizing uniform strain in the VE material (Eq. (18)) compared to the original detailed long duration (DLD) model presented in Section 4.

$$\gamma^{(n)} = u_d^{(n)} / d_v \tag{18}$$

It follows $a_j^{(n)}$ and $b_j^{(n)}$ in Eq. (8) are to be approximated by uniform values $a^{(n)}$ and $b^{(n)}$, respectively. Thus, it becomes

$$\tau^{(n)} + a^{(n)} D^{\alpha} \tau^{(n)} = G\left[\gamma^{(n)} + b^{(n)} D^{\alpha} \gamma^{(n)} \right] \tag{19}$$

where $a^{(n)}$ and $b^{(n)}$ are calculated using the average nodal temperature $\bar{\theta}^{(n)}$ of the VE material at time-step n. Therefore, Eq. (9) becomes

$$a^{(n)} = a_{ref} (\lambda^{(n)})^{\alpha}, \qquad b^{(n)} = b_{ref} (\lambda^{(n)})^{\alpha}, \qquad \lambda^{(n)} = \exp\left[- p_1 \left(\bar{\theta}^{(n)} - \theta_{ref} \right) / \left(p_2 + \bar{\theta}^{(n)} - \theta_{ref} \right) \right] \tag{20a-c}$$

Combining Eqs. (18) ~ (20) with the weight factors in Eq. (11) and by step-by-step integration scheme for Eq. (19), time-step shear stress $\tau^{(n)}$ can be calculated as:

$$\tau^{(n)} = \left\{ (u_d^{(n)} / d_v) G B^{(n)} + G b^{(n)} \sum_{i=1}^{N} w^i \gamma^{(n-i)} - a^{(n)} \sum_{i=1}^{N} w^i \tau^{(n-i)} \right\} \Big/ A^{(n)} \tag{21}$$

where

$$A^{(n)} = \left[(\Delta t)^{\alpha} + a^{(n)} w^{(0)} \right], \qquad B^{(n)} = \left[(\Delta t)^{\alpha} + b^{(n)} w^{(0)} \right] \tag{22}$$

Damper force $F_d^{(n)}$ can still be calculated using Eq. (14). However, the temperature rise $\Delta\theta^{(n)}$ and the dissipated energy $\Delta E_d^{(n)}$ are uniform throughout the VE material for a given time-step n, and are defined as:

$$\Delta\theta^{(n)} = \frac{\Delta E_d^{(n)}}{s_{VE} \rho_{VE}}, \qquad \Delta E_d^{(n)} = \left(\tau^{(n)} + \tau^{(n-1)} \right) \left(\gamma^{(n)} - \gamma^{(n-1)} \right) / 2 \tag{23a, b}$$

Finally, the temperature distribution of the VE damper will be calculated using the same principle presented in Eq. (16) but with temperature rise due to the dissipated energy in Eq. (23a). Therefore, Eq. (16a) becomes

$$\theta_j^{(n+1)} = \Delta\theta^{(n)} + \hat{\theta}_j^{(n)} \tag{24}$$

5.2 Analytical Verification

Damper 1 was analyzed using the SLD model and results were compared to those from experiment (Section 2) and the DLD model (Section 4). Temperatures using SLD model are compared to those from experiment (Fig. 20a) and DLD model (Fig. 20b). As seen, the SLD model agrees well to both experiment and DLD model.

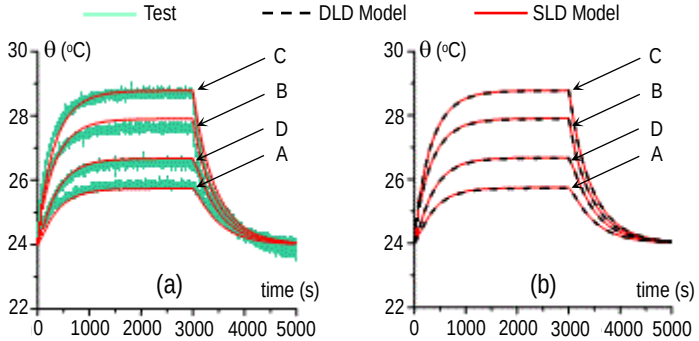

Fig. 20 – Comparison of temperatures of Damper 1:
(a) SLD model vs experiment, and; (b) SLD model vs DLD model

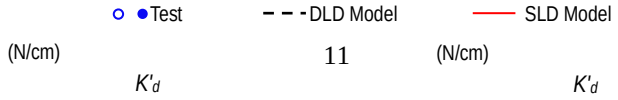

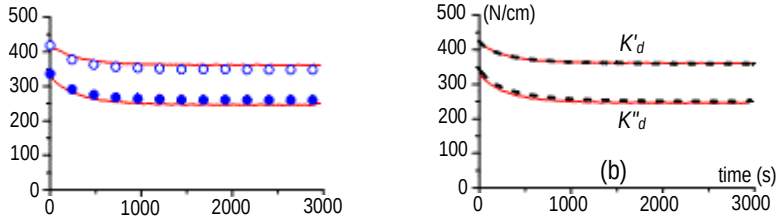

Comparison of K'_d and K''_d between the (a) SLD model and experiment, and (b) SLD model and DLD model are shown in Fig. 21, respectively. Obviously, the prediction of the SLD model has high accuracy even though it approximates uniform strain distribution.

5.3 Calculation Time

SLD model has an advantage over the DLD model in terms of calculation time since it approximates the strain distribution to be uniform throughout the VE material for every step.

Table 3 indicates the calculation time in the analysis of the different damper configurations (Section 3.4) using DLD and SLD models. Analyses were done by making a computer program in FORTRAN. The VE materials of Dampers 1 and 2 were divided into 16 elements each while for Damper 3 into 8 elements because it is thinner.

The ratio between the calculation time of SLD and DLD models clearly indicates a large improvement in analysis time. For Dampers 1 and 2, calculation time using SLD model is only 0.136 that of DLD model with temperature (Fig. 20b) and stiffness (Fig. 21b) in good agreement with the original DLD model.

In addition, the improvement in calculation time is dependent on the number of elements used. With lesser number of elements used for Damper 3, the calculation time improved lesser compared to Dampers 1 and 2.

Table 3 – Comparison of calculation time between DLD and SLD models

Damper	**Number of Elements**			**Calculation time (s)**		**SLD / DLD**
	Outer Plate	VE Material	Inner Plate	DLD Model	SLD Model	
1	4	16	2	2.42	0.33	0.136
2	4	16	2	2.42	0.33	0.136
3	4	8	2	1.39	0.28	0.201

6. Conclusions

This paper presented a 3D-FEM method analysis and a 1D-detailed long duration (DLD) model of VE damper considering heat generation, conduction and convection. In addition, a simplified long duration (SLD) model was proposed which idealized a uniform strain distribution. Results from SLD and DLD models were in good agreement, however, the former calculates faster than the latter.

The inclusion of the heat conduction and convection in the DLD and SLD models is their greatest advantage as it greatly defines the real behavior of VE damper when subjected to long duration loadings such as wind force. After long time of energy dissipation, the VE damper thermally reached steady-state and responded steadily.

7. References

[1] Kasai K, Munshi JA, Lai ML, Maison BF (1993): Viscoelastic Damper Hysteresis Model, Theory, Experiment, and Application. *ATC17-1 Seminar on Seismic Isolation, Passive Energy Dissipation and Active Control*, Applied Technology Council, **Vol 1.2**, 521-532

[2] Kasai K, Teramoto M, Okuma K, Tokoro K (2001): Constitutive Rule for Viscoelastic Materials Considering Temperature and Frequency Sensitivity (Part 1: Linear Model with Temperature and Frequency Sensitiveness). *Journal of Structural and Construction Enigneering (Transactions of AIJ)*, **543**, 77-86 (In Japanese).

[3] Kasai K, Sato D, Huang Y (2006): Analytical Methods for Viscoelastic Damper Considering Heat Generation, Conduction and Transfer under Long Duration Cyclic Load. *Journal of Structural and Construction Enigneering (Transactions of AIJ)*, **599**, 61-69 (In Japanese).

[4] Holman JP (1986): *Heat Transfer*. McGraw-hill, New York, 6th edition